Contents lists available at ScienceDirect

Organic Geochemistry

journal homepage: www.elsevier.com/locate/orggeochem

A rapid method for preparing low volume CH_4 and CO_2 gas samples for ^{14}C AMS analysis

Mary A. Pack [a,*], Xiaomei Xu [a], Massimo Lupascu [a], John D. Kessler [b], Claudia I. Czimczik [a]

[a] Department of Earth System Science, 2222 Croul Hall, University of California, Irvine, Irvine, CA 92697-3100, USA
[b] Department of Earth & Environmental Sciences, University of Rochester, Rochester, NY 14627, USA

ABSTRACT

^{14}C measurements of CH_4 in environmental samples (e.g. soil gas, lake water, gas hydrates) can advance understanding of C cycling in terrestrial and marine systems. The measurements are particularly useful for detecting the release of old C from climate sensitive environments such as peatlands and hydrate fields. However, because ^{14}C CH_4 measurements tend to be complex and time consuming, they are uncommon. Here, we describe a novel vacuum line system for the preparation of CH_4 and CO_2 from environmental samples for ^{14}C analysis using accelerator mass spectrometry (AMS). The vacuum line is a flow-through system that allows rapid preparation of samples (1 h for CH_4 and CO_2, 30 min for CH_4 alone), complete separation of CH_4 and CO_2 and is an easy addition to multipurpose CO_2 vacuum lines already in use. We evaluated the line using CH_4 and CO_2 standards with different ^{14}C content. For CH_4 and CO_2, respectively, the total line blank was 0.4 ± 0.2 and 1.4 ± 0.6 µg C, the ^{14}C background 51.1 ± 1.2 and 48.4 ± 1.5 kyr and the precision (based on pooled standard deviation) 0.9‰ and 1.3‰. The line was designed for sample volumes of ca. 180 ml containing 0.5–1% CH_4 and CO_2, but can be adjusted to handle lower concentration and larger volume samples. This rapid and convenient method for the preparation of CH_4 and CO_2 in environmental samples for ^{14}C AMS analysis should provide more opportunities for the use of ^{14}C CH_4 measurements in C cycle studies.

1. Introduction

CH_4 is an atmospheric trace gas with a warming potential $28\times$ that of CO_2 over a 100 yr timespan (Myhre et al., 2013) as well as a precursor for tropospheric O_3 (Fiore et al., 2012). Since the industrial revolution (1750–2010), CH_4 concentration has increased from 700 ± 25 to 1795 ± 18 ppb (Prather et al., 2012). Global annual CH_4 emissions are reasonably well constrained from 'top-down' observations of changing atmospheric lifetime and abundance (Spahni et al., 2011; Prather et al., 2012) and emission inventories (Yusuf et al., 2012). In contrast, the geographical distribution and interannual variability of individual CH_4 emission sources are poorly understood (Dlugokencky et al., 2011) and remain major uncertainties in projections of future atmospheric CH_4 levels and surface temperatures (Heimann and Reichstein, 2008). A better understanding of C cycling in terrestrial and marine systems should improve estimations of individual CH_4 emission sources and our ability to predict future CH_4 levels.

Isotope analysis is a powerful tool for advancing understanding of C cycling (e.g. Kvenvolden, 1995; Sansone et al., 2001; Steinmann et al., 2008). In terrestrial and marine systems, CH_4 is produced biologically via the microbial decomposition of organic C under anaerobic conditions, thermogenically deep underground and abiotically in cold seep environments (Le Mer and Roger, 2001; Reeburgh, 2007). The CH_4 produced can be released to the atmosphere, stored (e.g. coal beds and CH_4 hydrates) or consumed under both aerobic and anaerobic conditions. Its stable isotope content ($^{13}C/^{12}C$, $^{2}H/^{1}H$) can distinguish microbial from thermogenic sources and between different microbial CH_4 production pathways (Whiticar, 1999; Townsend-Small et al., 2012), as well as the extent of methane oxidation (Alperin et al., 1988; Kessler et al., 2006). Radiocarbon ($^{14}C/^{12}C$) measurements can provide additional information on CH_4 sources and determine the age of contributing C pools (i.e. source age; Kessler et al., 2005; Garnett et al., 2013).

^{14}C is produced in the atmosphere by cosmic radiation, oxidized to $^{14}CO_2$ and incorporated into the global C cycle. Because ^{14}C decays over time, C isolated from the atmosphere in terrestrial and marine systems (i.e. stored C) has a lower $^{14}C/^{12}C$ ratio than atmospheric CO_2 or C recently fixed by photosynthesis. CH_4 (or

---

CO_2) originating from material that has been isolated/stored and has a low $^{14}C/^{12}C$ ratio is termed old and, when the $^{14}C/^{12}C$ ratio approaches zero, the term dead/fossil is applied. Oppositely, CH_4 (or CO_2) produced from organic material with a $^{14}C/^{12}C$ ratio similar to the present atmospheric $^{14}C/^{12}C$ CO_2 ratio is referred to as modern or young.

^{14}C is of particular interest for understanding C cycle feedbacks to climate change because it can measure source age. The rapid cycling of C between plants (terrestrial vegetation and aquatic phytoplankton) and microbes has a near net zero effect on the atmospheric C pool (Trumbore, 2009). On the other hand, the decomposition of older and fossil C that has not been part of the active C cycle for millennia results in a net flux of C to the atmosphere and a positive warming feedback. Thus, measurement of ^{14}C CH_4 (and ^{14}C CO_2) can help detect the release of old and fossil C to the atmosphere in addition to advancing understanding of C cycling. Unfortunately, because ^{14}C CH_4 measurements tend to be expensive, complex and time consuming, their use as a tool for C cycle investigations is limited.

There are four general techniques for preparing CH_4 from environmental samples for isotope (^{14}C and ^{13}C) analysis. They are often used to prepare sample CO_2 simultaneously with CH_4 and generally take > 1 h. The processing time does not include the reduction of CO_2 to graphite (graphitization), which is required for most ^{14}C accelerator mass spectrometry (AMS) analyses. The most common technique is a flow-through system where a carrier gas (He and/or O_2) is used to carry sample gas through a system at atmospheric pressure (e.g. Chanton et al., 1992; Pohlman et al., 2000, 2009). The sample gas is carried through a series of cryogenic traps and a combustion tube packed with an oxidizing catalyst (CuO or Pt wire) and heated to > 800 °C in a tube furnace. The traps allow separation of sample CH_4 from CO_2 and other impurities, while the combustion tube converts the CH_4 to CO_2. A portion of the resulting CO_2 is analyzed for ^{13}C via isotope ratio MS (IRMS), while the remaining CO_2 is reduced to graphite for ^{14}C analysis using AMS. In most cases, the sample CO_2 is recovered after the CH_4 and is also analyzed for ^{14}C and ^{13}C.

In a second and similar technique, a sample flask is attached to a vacuum line system composed of cryogenic traps and a combustion tube and the sample is carried through the line at reduced pressure (e.g. Lowe et al., 1991; Garnett et al., 2011). This technique utilizes the pressure difference between the sample flask and vacuum line system to move sample through the line and does not require a carrier gas. Thirdly, CH_4 can be separated from CO_2 and prepared for isotopic analysis using custom-made gas chromatography systems (e.g. Aravena and Wassenaar, 1993). More recently, a fourth technique was developed that recirculates sample gases mixed with a carrier gas through cryogenic traps and a combustion tube at reduced pressure (Kessler and Reeburgh, 2005). The recirculating procedure allows complete recovery of sample CH_4 and thereby eliminates any ^{13}C CH_4 and ^2H CH_4 isotope fractionation.

Three of the above methods cryogenically separate CH_4 from CO_2; however, careful consideration is needed with the technique because a portion of CH_4 may be condensed with CO_2 at liquid N_2 temperature (LN_2, −196 °C) if the partial pressure of CH_4 is too high (Clymo and Bryant, 2008; Garnett et al., 2011). Other than cryogenic separation, there are two common techniques for isolating CH_4 from CO_2. The addition of a base such as KOH to a sample will sequester the CO_2 in solution as CO_3^{2-} (e.g. Chasar et al., 2000). After extraction of CH_4, acidification of the sample releases the CO_2, which can then be purified and analyzed for ^{14}C and ^{13}C. This is an effective technique, but special attention must be paid to ensure the base is free of CO_3^{2-} and hydrocarbons and does not contribute to the method blank. Passing sample gases through certain types of molecular sieve can also pull out CO_2 and separate it from CH_4 (Garnett et al., 2011). The CO_2 can be retrieved later by heating the molecular sieve. This is also an effective technique, but molecular sieves, if not properly treated, can lend themselves to memory effects and high blanks (e.g. Hardie et al., 2005). Overall, these alternative methods require greater time commitment per sample than cryogenic separation because of the effort required to maintain a low background.

A few of the reported techniques also target the removal of CO, an impurity than can alter ^{14}C and ^{13}C CH_4 values for samples with sufficient CO concentration. An inline trap with Schütze reagent or Sofnocat 423 that converts CO to CO_2 at room temperature (e.g. Lowe et al., 1991; Chanton et al., 1992; Petrenko et al., 2008) is commonly used for this purpose. Once oxidized to CO_2, the CO can be cryogenically separated from CH_4. Another option used for CO removal is catalytic oxidation over CuO at 290 °C (Kessler and Reeburgh, 2005). Compared with Schütze reagent, CuO and Sofnocat 423 are safer to handle because they are less reactive and pose fewer health risks [based on material safety data sheet (MSDS) numbers]. Also, CuO can be easily reactivated by baking under air at 900 °C, whereas there are no common methods for regeneration of Schütze reagent or Sofnocat 423. Isotopic analysis of the CO-derived CO_2 is common with large volume air samples (e.g. Klouda and Connolly, 1995), but to the best of our knowledge, not with the terrestrial and marine studies that are the focus here.

Here we present a novel flow-through vacuum line system for preparing CH_4 and CO_2 from low volume environmental samples for ^{14}C AMS and ^{13}C IRMS analysis. The system utilizes a carrier gas and cryogenically separates CH_4 from CO_2, but unlike previous methods, maintains low pressure through the line to ensure complete CH_4/CO_2 separation. Further, the system (i) allows rapid recovery of both CH_4 and CO_2 (1 h per sample, 30 min for CH_4 alone), (ii) is an easy addition to multipurpose CO_2 vacuum lines already in use, (iii) includes a 290 °C oven with CuO that efficiently oxidizes CO to CO_2 and (iv) employs the sealed tube Zn graphitization method (Xu et al., 2007) so that the 0.5–1 h processing time includes sample purification and combustion along with graphitization preparation. Our aim with this flow-through line was to provide a method for the sequential preparation of CH_4 and CO_2 in environmental samples for ^{14}C AMS analysis that is rapid and convenient and thereby expands the use of ^{14}C measurements in C cycle studies.

2. Methods

2.1. Flow-through vacuum line

The line has 3 stages (Fig. 1). In stage 1, CO_2 and CO, after catalytic oxidation to CO_2, are separated from CH_4 in individual cryogenic traps [1–8] (numbers in square brackets refer to those in Fig. 1). In stage 2, the purified CH_4 is combusted to CO_2 [9]. In stage 3, the sample CO_2 and CH_4-derived CO_2 are recovered, quantified and prepared for graphitization [10–18]. When not in use, stages 1 and 2 are kept at atmospheric pressure and temperature with a flow of ultra-zero (UZ) air (< 5 ml/min). The UZ airflow prevents particulates and gases in ambient air from entering the line and maintains a low line blank. This is the same air used for the carrier gas in the system and is cleaned with an inline Ascarite filter [2] just after exiting its tank [1]. Stage 3 is a multipurpose CO_2 vacuum line kept under vacuum when not in use. Altogether, the flow-through line combines techniques from three previous studies: a low pressure flow-through system for pure CH_4 samples (Pack et al., 2011), a CuO oven at 290 °C to catalytically oxidize CO to CO_2 (Kessler and Reeburgh, 2005) and a multipurpose CO_2 vacuum line (Xu et al., 2007).
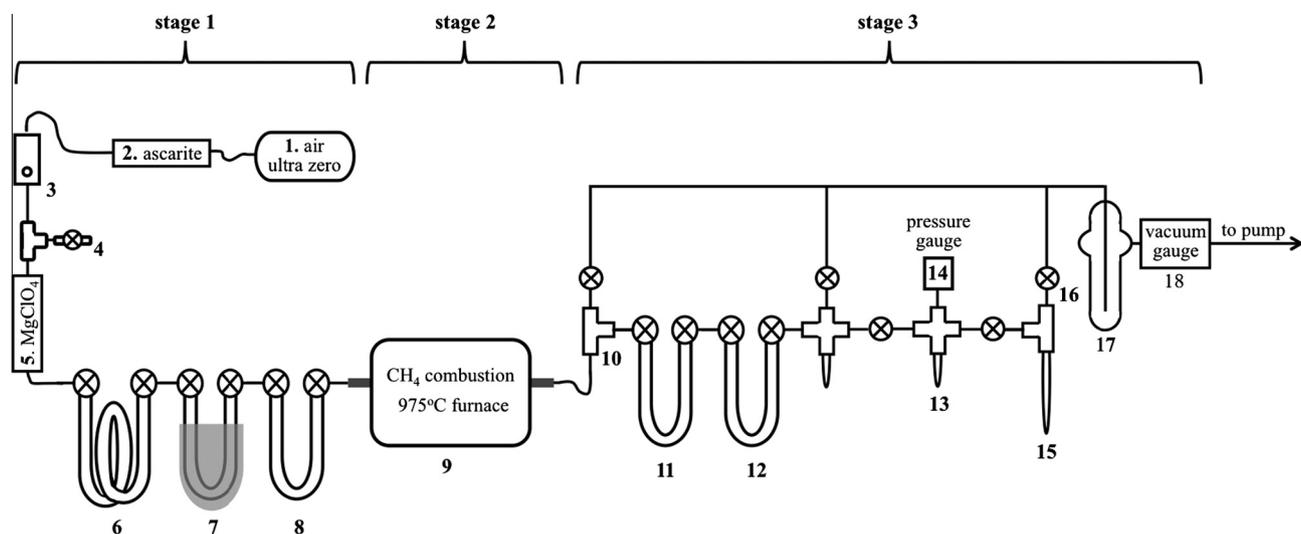
Fig. 1. Diagram of flow-through vacuum line (not to scale): [1] Tank of UZ air with a low-end pressure of 35 kPa (gauge), [2] Pyrex glass tube (9 mm outer diameter, OD × 25 cm) packed with Ascarite, [3] flowmeter (0–50 ml/min), [4] Swagelok Ultra-torr tee (6.35 mm, #SS-4-UT-3) and needle valve (6.35 mm tube fittings, #SS-1RS4) with septum for injection, [5] Pyrex glass tube (9 mm OD × 15 cm) packed with $Mg(ClO_4)_2$, [6] Pyrex glass multi-loop trap (9 mm OD, 9 cm × 18 cm with non-rotating stem valves) packed with glass ribbon and cooled with LN_2, [7] Pyrex glass U trap packed with CuO, wrapped with heat tape, heated to 290 °C with a variac transformer and monitored with a thermocouple, [8] Pyrex glass U trap packed with glass beads and cooled with LN_2, [9] Lindberg/Blue Furnace (Thermo Scientific #TF55050A) at 975 °C with a quartz combustion tube (25 mm OD × 40 cm, tapered to 9 mm OD at both ends) packed with CuO, [10] Swagelok Ultra-torr tee where the tube furnace outlet is attached to stage 3, [11] Pyrex glass U trap packed with glass beads and cooled with a dry ice-EtOH slurry, [12] Pyrex glass U trap packed with glass beads and cooled with LN_2, [13] calibrated volume reservoir, [14] MKS Inst. BaratronType 122A absolute pressure gauge with PRD-D-1 digital readout, [15] reaction tube for graphitization, [16] vacuum valve – plug valve separating the line from the vacuum pump, [17] vacuum trap cooled with LN_2 to prevent back flow of vacuum pump oil, [18] Granville-Phillips series 375 convectron vacuum gauge; ⊗ represents either plug or stem valves. Glass or quartz wool and steel wool are placed on top of all the trap packing to prevent movement in response to pressure change. The U traps [7, 8, 11, 12] are all 9 mm OD, 7.5 cm × 18 cm, and have non-rotating stem valves. The connecting tubing for [1]–[4] and [4]–[6], [8]–[10] is 6.35 mm and 3.18 mm OD, respectively, high temperature Teflon tubing (Cole–Parmer).

2.2. Procedures

2.2.1. Daily setup

The oven for CO oxidation [7] and the tube furnace for CH_4 combustion [9] are turned on and allowed to thermally equilibrate to 290 °C and 975 °C, respectively, for 1 h. During this time, a dewar flask with LN_2 is added to the vacuum trap [17], stage 3 (the multipurpose vacuum line) is pumped to baseline (1–2 m torr) and a dry ice–EtOH slush is added to the water trap [11]. After this warm up period, the combustion tube [9] outlet is attached to an Ultratorr fitting [10] on the multipurpose vacuum line, connecting stages 1 and 2 to stage 3. The pressure through the line is monitored with a pressure gauge [14] in the middle of stage 3, and a vacuum gauge [18] at the end of stage 3. Pressures reported in torr are read at the pressure gauge [14], while those reported in m torr are read from the vacuum gauge [18].

2.2.2. Sample introduction

The entire line from trap [6] to the vacuum valve [16] is filled with 500 torr UZ air and evacuated (3×). This cleans out the traps and ovens, helps keep the background value low and reduces the chance of memory effects. The line will quickly evacuate to 300–600 m torr and then slowly stabilize to a pressure dependent on the amount of O_2 released by the combustion tube [9] (its CuO packing is decomposed to Cu and O_2 when heated to > 600 °C). Evacuating to a pressure < 300–600 m torr does not improve the line blank and pumps O_2 out of the combustion tube [9]. This pressure may vary with other systems, depending on the setup of the vacuum line and position of the vacuum gauge relative to the vacuum pump. After the third evacuation, the line is left open to the vacuum pump (i.e. valve [16] is left open) and UZ air at ca. 10 ml/min is supplied to the line at the flow meter [3]. This creates a continuous flow of UZ air through the line from the flow meter to the vacuum pump with a line pressure of ca. 1 torr. Next, LN_2

dewar flasks are added to traps [6, 8, 12]. Finally, sample gas is introduced to the line at the injection port [4] via a syringe. A needle valve behind the injection port is used to keep the injection flow < 105 ml/min. Without the needle valve, the low line pressure (ca. 1 torr) would rapidly pull the sample gases out of the syringe and into the line. After sample introduction is complete, the needle valve is fully opened.

2.2.3. Sample purification, separation and combustion

The injected sample gas is carried with the UZ airflow through a series of traps. Starting in stage 1, it passes through an inline trap packed with $Mg(ClO_4)_2$, which dries the sample. Next, the sample enters a multi-loop trap cooled with LN_2 [6], where sample CO_2 is frozen out. The sample then passes through two U traps: one packed with CuO and heated to 290 °C [7], followed by another cooled with LN_2 [8]. Here, CO is oxidized to CO_2 and then frozen down. The purified sample continues to stage 2, passes through a 975 °C combustion tube [9], and the sample CH_4 is converted to CO_2 and water. O_2 for combustion is supplied by the continuous flow of UZ air (ca. 20% O_2) and the CuO packing in the combustion tube. The combusted sample enters stage 3, where the water is frozen down with a dry ice-EtOH cooled trap [11], the CH_4-derived CO_2 is recovered in a LN_2 cooled trap [12] and the remaining sample and UZ air (mostly N_2 and O_2) are pumped away. This whole process is allowed to run for 10 min to ensure that all sample CH_4 and CO_2 are recovered.

2.2.4. Preparation of CO_2 for graphitization

The left valve on trap [11] is closed after the 10 min run, which again separates stage 3 from stages 1 and 2, and allows the residual UZ air in stage 3 to be pumped out. While stage 3 pumps to baseline, the valves on the trap holding the sample CO_2 [6] are closed and the trap is left cold with LN_2 (it is important to keep this trap cold – see the safety note below). Oppositely, the valves on the trap

holding the CO-derived CO_2 [8] are left open, the LN_2 dewar is removed from the trap (it is important that the valves on the trap are left open-see the safety note below) and the CO_2 is allowed to volatize (this CO_2 is pumped away later).

Once stage 3 has been pumped to baseline, the trap with the CH_4-derived CO_2 [12] is isolated, the trap's LN_2 dewar is removed and the CO_2 is cryogenically transferred to a known volume reservoir [13] and quantified by measuring the CO_2 pressure [14]. An aliquot of the quantified CO_2 may be taken for ^{13}C IRMS analysis, while the remaining CO_2 is prepared for ^{14}C AMS analysis as described by Xu et al. (2007) using the sealed tube Zn graphitization method.

Lastly, the sample CO_2 that was isolated in trap [6] is transferred to trap [12] for quantification and graphitization. To start, stage 3 and stages 1–2 are evacuated to baseline and 200–500 m torr, respectively, while leaving trap [6] isolated (this pumps away the CO-derived CO_2). After replacing the LN_2 dewar on trap [12], the valves on trap [6] are opened, and the continuous flow of UZ air through the line resumes. The LN_2 dewar on trap [6] is removed, the sample CO_2 is volatized and carried with the UZ airflow to trap [12]. This transfer is given 10 min to come to completion, after which the sample CO_2 in trap [12] is quantified and prepared for graphitization as described above.

2.2.5. Safety note

It is important that any trap cooled with LN_2 is evacuated before or left open (to provide added volume for gas expansion) when the LN_2 is removed. A portion of the N_2 and O_2 in the UZ air and O_2 released from the CuO in the combustion tube [9] can condense in any trap cooled with LN_2 during sample processing. If a LN_2 cooled trap warms without prior evacuation and its valves are closed, the pressure from the expanding N_2 and O_2 gases could cause the trap to explode. For the same reason, when shutting down the vacuum line at the end of the day, it is important to remove the LN_2 dewar from the vacuum trap [17] and pump out any N_2 or O_2 condensed in the trap. An added safety concern is that condensed O_2 can combust if exposed to sufficient hydrocarbons along with a spark. These conditions are unlikely with the vacuum line system and low hydrocarbon samples described here. Further, when O_2 condenses in a trap it forms a blue liquid and we have not observed this under the operating conditions described above.

2.2.6. Line maintenance

The Ascarite filter [2], $Mg(ClO_4)_2$ filter [5] and CuO packing in the 290 °C oven [7] for CO oxidation need to be monitored and replaced or regenerated over time. The frequency at which these packings need to be changed depends on the number of samples processed and their composition (e.g. CO and water content, volume). The Ascarite and $Mg(ClO_4)_2$ packing change in physical appearance when they become saturated with CO_2 or water, respectively: the Ascarite lightens in color and dries out, while the $Mg(ClO_4)_2$ turns opaque and looks wet. The efficiency of the CO 290 °C oven should be monitored with dilute CO run through the line and, when found to be less efficient, the CuO packing should be regenerated as described below.

2.3. Experiments

Six pure standards (N_2 gas, CH_4 gas, bone dry CO_2 gas, and CO_2 from OX1, coral and calcite solids; see Tables 1 and 2 for ^{14}C and ^{13}C content) were prepared on the flow-through vacuum line to evaluate the total C blank, modern ^{14}C background, combustion efficiency, accuracy and precision for the preparation of both CH_4 and CO_2. All ^{14}C AMS and ^{13}C IRMS analyses were carried out at the W.M. Keck Carbon Cycle AMS (KCC AMS) facility at the University of California, Irvine (Southon and Santos, 2004, 2007).

Table 1
Summary of measured ^{14}C from ca. 0.5–1 mg C aliquots of pure CH_4 and CO_2 standards prepared on the flow-through vacuum line and their expected values (age = radiocarbon age in kyr; SD, ± 1σ standard deviation).

Standard			Measured ^{14}C				Expected ^{14}C	
Name	Type	n	FM	SD	Age	SD	FM	Age
Dead CH_4	Gas	8	0.0016	0.0003	51.9	1.8	0.0025	48.1[a]
BD-CO_2	Gas	2	0.0024	0.0005	48.4	1.5	0.0019	50.3
OX1-CO_2[b]	Solid	6	1.0395	0.0020			1.0398[c]	
Coral-CO_2	Solid	3	0.945	0.0027			0.9440[d]	

[a] Values from dead CH_4 gas prepared on the Kessler and Reeburgh (2005) vacuum line.
[b] We use the new notation (OX1) based on Mook and Van Der Plicht (1999) rather than the older notation HOx-1.
[c] Currie and Polach (1980), Stuiver and Polach (1977).
[d] Hinger et al. (2010).

Table 2
Summary of measured ^{13}C from ca. 0.5–1 mg C aliquots of pure CH_4 and CO_2 standards prepared on the flow-through vacuum line and their expected values (SD, ± 1σ standard deviation).

Standard			Measured ^{13}C		Expected ^{13}C	
Name	Type	n	‰	SD	‰	SD
Dead CH_4	Gas	2	−36.27	0.08	−36.35[a]	0.05
OX1-CO_2	Solid	2	−19.0	0.1	−19.0[b]	
Calcite-CO_2	Solid	3	2.87	0.16	3.15[c]	0.39

[a] Values from dead CH_4 gas prepared on the Kessler and Reeburgh (2005) vacuum line.
[b] Currie and Polach (1980), Stuiver and Polach (1977).
[c] Unpublished data from Ellen R. Druffel's Lab at the University of California, Irvine.

2.3.1. Line total C blank

The N_2 (15–185 ml) was drawn from a UHP N_2 gas cylinder through a soda lime trap (to remove any residual CO_2) using a 60 ml syringe. It was then introduced to the flow-through line and treated as a sample. The amount of C in the traps where sample CO_2 (Fig. 1, No. 6) and CH_4 (Fig. 1, No. 12) freeze down was considered to be the total C line blank for each species.

2.3.2. ^{14}C blank, efficiency, accuracy and precision for CH_4

The CH_4 (0.1–3 ml) was drawn from a UHP CH_4 gas cylinder with a 5 ml syringe and treated as a sample. The CH_4 gas was derived from a fossil source and is therefore ^{14}C-free (dead). Several aliquots of the CH_4 were prepared by J. Kessler's Lab using established vacuum line techniques (Kessler and Reeburgh, 2005) and the ^{14}C and ^{13}C contents of the resulting CO_2 were measured at the KCC AMS Facility. The measurements confirmed that the CH_4 gas was dead and provided data for an inter-laboratory comparison. The amount of CH_4 recovered as CO_2 on the line was used to determine the line's combustion efficiency, while the ^{14}C and ^{13}C values of the recovered CO_2 were used to evaluate the line's modern ^{14}C background and the ^{13}C accuracy and precision for CH_4.

2.3.3. ^{14}C blank, efficiency, accuracy and precision for CO_2

CO_2 from a bone dry CO_2 (BD-CO_2) gas cylinder was stored in 120 ml glass serum bottles (Wheaton Scientific #223747) with butyl rubber stoppers (Bellco Glass #2048-11800). Aliquots (0.1–2 ml) were drawn from the storage bottles via a 3 ml syringe and introduced to the line. The OX1 (NIST, SRM 4990 B) was combusted to CO_2 in sealed quartz tubes and cryogenically purified on a vacuum line (see Xu et al., 2007). A 20 ml syringe was used to draw the OX1-CO_2 (1–2 ml) from the vacuum line and introduce it to the flow-through line. The amount of CO_2 recovered compared with the OX1-CO_2 introduced was used to calculate the line's

CO_2 recovery. Coral (an in-house standard from E. Druffel's lab) and calcite standards (ca. 10 mg fine powder) were acidified with 0.8 ml H_3PO_4 (85%) in 3 ml evacuated glass vials with septa and heated (70 °C, 2 h). The resulting coral and calcite CO_2 was drawn directly from the glass vials using a 5 ml syringe and injected into the line. Because the BD-CO_2 gas is nearly dead, it was used for the line's modern ^{14}C CO_2 background evaluation, while the ^{14}C and ^{13}C values for the CO_2 from the solid standards were used to evaluate the accuracy and precision of CO_2 prepared on the line.

Note that ^{14}C background determined from ^{14}C dead standards represents the amount of modern C contaminating samples prepared on the line and does not include ^{14}C dead/fossil contaminants (i.e. ^{14}C dead contamination would not show when analyzing a dead C standard). We did not evaluate fossil background in the study because the samples/standards used were 0.5–1 mg C and fossil background only becomes important with samples < 0.1 mg C (Santos et al., 2007).

2.3.4. Separation of CH_4 and CO_2

Mixed standards were used to evaluate the ability of the flow-through vacuum line to separate sample CO_2 and CH_4. Standards were made by adding 1–2 ml OX1-CO_2, 2–4 ml dead CH_4 and 180 ml UHP N_2 to evacuated 120 ml glass serum bottles sealed with blue butyl stoppers. Mixed standard was removed from a bottle and injected into the line in three aliquots using a 60 ml syringe. The rate at which the mixed standards were injected was varied to test the separation of CO_2 and CH_4 at different injection flow rate. We purposely chose to mix modern OX1-CO_2 with dead CH_4 so that the CH_4 and CO_2 would have a 1000-fold difference in ^{14}C content and provide a sensitive test for the separation of the two gases.

2.3.5. CO oxidation efficiency

Both pure and diluted CO were used to evaluate the oxidation efficiency of the CO oven (Fig. 1, No.7). Pure CO from a UHP CO gas cylinder was either stored in 120 ml evacuated glass serum bottles with butyl rubber stoppers or diluted in the bottles with 2 ml pure CO in 180 ml UHP N_2 (ca. 1% CO). Pure CO (1.6–2.6 ml) and dilute CO (14–31 ml) were removed from their respective bottles via 5 or 60 ml syringes, and injected into the flow-through vacuum line. CO that is not oxidized in the CO oven (Fig. 1, No. 7) cannot freeze down in the subsequent trap (Fig. 1, No. 8). It can therefore continue down the line, be oxidized to CO_2 in the 975 °C combustion tube (Fig. 1, No. 9) and freeze down where CH_4-derived CO_2 is normally trapped (Fig. 1, No. 12). Thus, the amount of CO_2 in the CO-derived CO_2 trap (Fig. 1, No. 8) compared with that in the CH_4-derived CO_2 trap (Fig. 1, No. 12) was used to determine the CO oven oxidation efficiency. We varied the rate at which the CO was injected into the line and the temperature of the CO oven to test the oxidation efficiency under different conditions.

3. Results and discussion

3.1. Total C line blanks, combustion efficiency and ^{14}C background

The total C line blank was 0.0004 ± 0.0002 mg C and 0.0014 ± 0.0006 mg C for CH_4 and CO_2, respectively ($n = 7$). There was a large error associated with these values because they were close to the detection limit of the pressure gauge (Fig. 1, No. 14) in the calibrated volume reservoir (Fig 1, No. 13), but the values were still < 0.2% of a 1 mg C sample. The line's CH_4 combustion efficiency was 100.9 ± 3.6% ($n = 8$), while its CO_2 recovery was 101.5 ± 1.6% ($n = 5$).

The line's modern ^{14}C background measured from 0.5–1 mg C aliquots of dead CH_4 and BD-CO_2 prepared on the line (Table 1)

was satisfactory (i.e. < 0.0037 FM or > 45 kyr; fraction modern [FM] and ^{14}C age [kyr] as defined by Stuiver and Polach, 1977). Also, the CH_4 values were comparable with aliquots of the same CH_4 gas prepared on the Kessler and Reeburgh (2005) vacuum line (Table 1). Because the BD-CO_2 gas standard was nearly (but not completely) dead, it had an expected ^{14}C content of 0.0019 ± 0.0001 FM (50.3 ± 0.3 kyr, $n = 1$, instrument precision) instead of the ca. 0.0016 ± 0.0004 FM (51.8 ± 1.7 kyr, $n = 277$; Khosh et al., 2010) routinely measured for dead coal standards at the KCC AMS facility using sealed tube Zn graphitization. The CH_4 and CO_2 modern ^{14}C backgrounds were subtracted from sample and standard ^{14}C values during the routine data reduction of raw ^{14}C AMS data (e.g. Santos et al., 2007).

3.2. Accuracy and precision

The ^{13}C values from the dead CH_4 gas prepared on the flow-through vacuum line were within the analytic error (± 1σ) of the same CH_4 prepared on the Kessler and Reeburgh (2005) vacuum line (Table 2). As commercially available CH_4 is generally prepared from fossil sources, we were unable to locate a CH_4 standard with a modern level of ^{14}C. The ^{14}C and ^{13}C values from the CO_2 standards (BD-CO_2 gas, and CO_2 from the OX1, coral and calcite solids) prepared on the line were within the analytic error of their expected values (Tables 1 and 2).

The precision for CH_4 and CO_2 prepared on the line, based on replicate measurements of standards and samples, is shown in Table 3. The pooled standard deviation for ^{14}C measurements was 0.0009 FM (0.9‰, $n = 5$) and 0.0013 FM (1.3‰, $n = 11$) for CH_4 and CO_2, respectively, similar to the 2–3‰ long term relative error achieved at the KCC AMS Facility using sealed tube Zn graphitization (Xu et al., 2007). For the ^{13}C measurements, the pooled standard deviation was 0.06‰ ($n = 15$) and 0.13‰ ($n = 10$) for CH_4 and CO_2, respectively, similar to the 0.1–0.15‰ precision routinely achieved with gas bench ^{13}C IRMS analysis at the KCC AMS Facility.

3.3. Separation of CH_4 and CO_2

The multi-loop trap (Fig. 1, No. 6) is a critical component in the line for efficiently freezing down CO_2 and separating it from CH_4, but was not present in our original design. Initially, sample CO_2 was frozen down alongside the CO-derived CO_2 in the U trap following the CO oven (Fig. 1, No. 8) and was not analyzed. The dead CH_4 in OX1:CH_4 mixed standards prepared on the original line averaged 0.0166 ± 0.0239 FM (39.0 ± 10.3 kyr, $n = 6$) and had a higher ^{14}C content than aliquots of pure dead CH_4 prepared on

Table 3
Average values and standard deviation (SD, ± 1σ) from replicate ^{14}C AMS and ^{13}C IRMS measurements of standards and samples prepared on the flow-through vacuum line.

Sample	n	^{14}C (FM)	SD	$\Delta^{14}C$ (‰)	SD	n	$\delta^{13}C$ (‰)	SD
Bog S4_CH_4[a]	2	1.0450	0.0000	37.3	0.1	2	−60.3	0.1
Bog S5_CH_4[a]	3	1.0656	0.0015	57.7	1.5	3	−56.6	0.2
Dead CH_4	–	–	–	–	–	10	−36.3	0.1
Bog S4_CO_2[a]	2	0.9408	0.0011	−66.3	1.1	2	−4.0	0.1
Bog S5_CO_2[a]	3	1.0193	0.0028	11.7	2.8	3	−8.9	0.2
Calcite-CO_2	–	–	–	–	–	2	2.9	0.2
OX1-CO_2	6	1.0395	0.0020	31.7	2.1	2	−19.0	0.1

[a] Gas samples collected from collapsed bog sites between June 16 and September 13, 2011 in the Alaska Peatland Experiment sites (APEX, 64.70°N, −148.32°W) near the Bonanza Creek Experimental Forest on the Tanana Valley flood plain in interior Alaska, USA (http://www.lter.uaf.edu/). The samples were collected by Merritt R. Turetsky's lab group in the Department of Integrative Biology, University of Guelph, Canada. The data are used here solely for the purpose of precision tests.
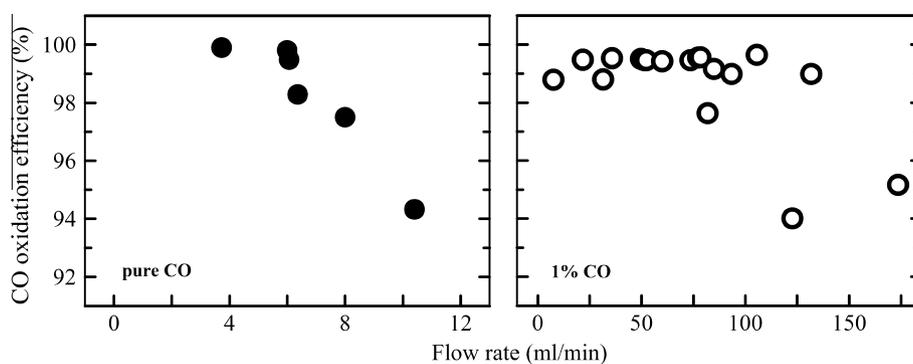
Fig. 2. ^{14}C age values for CH_4 from OX1:CH_4 mixed standards and pure dead CH_4 standard prepared on the flow-through vacuum line at different injection flow rate before and after the installation of the multi-loop trap for CO_2 removal (Fig. 1, No. 6).

the line (0.0016 ± 0.0003 FM, 51.9 ± 1.8 kyr, n = 8, Table 1). The ^{14}C content of dead CH_4 in the mixed standards also rose with faster injection flow rate on the original line: the content for slow flow rate (< 11 ml/min) was 0.0028 ± 0.0001 FM (47.1 ± 0.7 kyr, n = 2), but 0.0234 ± 0.0276 FM (34.9 ± 10.5 kyr, n = 4) for fast flow rate (Fig. 2). These data indicate that the U trap for CO-derived CO_2 alone (Fig. 1, No. 8) was inefficient for trapping the OX1-CO_2, and allowed a small portion of the OX1-CO_2 to continue down the line and contaminate the CH_4-derived CO_2 (trapped in No. 12, Fig. 1). Less than 1% of the OX1-CO_2 escaping the CO-derived CO_2 trap (Fig. 1, No. 8) could explain the elevated ^{14}C CH_4 values for the mixed standards. After the more efficient multi-loop trap (Fig. 1, No. 6) was installed to capture CO_2, the ^{14}C content of CH_4 in the OX1:CH_4 mixed standards dropped to a satisfactory background of 0.0018 ± 0.0002 FM (50.8 ± 1.0 kyr, n = 10) and did not change with injection flow rate (tested up to 120 ml/min, Fig. 2).

The ^{14}C values for the OX1-CO_2 in OX1:CH_4 mixed standards confirmed the complete separation of CH_4 and CO_2 in the line, but were not straightforward. The ^{14}C OX1-CO_2 value from one mixed standard processed the same day it was prepared was 1.0389 ± 0.0014 FM (n = 1, instrument precision, Table 4) and was not statistically different from the expected value of 1.0398 FM (Table 1). However, the ^{14}C OX1-CO_2 values from mixed standards stored for 0.5–8.7 months ranged from 1.0340 ± 0.021 FM (n = 8) to 1.0191 ± 0.0023 FM (n = 1, instrument precision) and decreased with storage time (Table 4). The ^{14}C CH_4 values in the same mixed standards were consistent, comparable with pure dead CH_4 prepared on the line and gave no indication of incomplete separation or change during storage. Together, these data point to a storage problem with the mixed standards where (i) a small amount of

dead CH_4 gas was biologically or chemically converted to CO_2 or (ii) a small amount of dead CO_2 was released from the butyl stoppers.

The same trend of decreasing ^{14}C-OX1 content with longer storage time was observed with OX1-CO_2 in N_2 standards stored in glass serum bottles with butyl rubber stoppers (Table 4). We thus suspect that the low ^{14}C content of the OX1-CO_2 in the stored CH_4:OX1 mixed standards was due to outgassing of dead CO_2 from the butyl rubber stoppers. Butyl rubber stoppers are manufactured from ^{14}C dead material and may outgas under certain conditions (Gao et al., 2014). Outgassing of old CO_2 can affect modern samples, so further experiments are necessary to identify stopper pre-treatment that reduces outgassing, or an alternative long term storage vessel.

3.4. Co oxidation efficiency

The oxidation efficiency of CO in the line was high both for pure CO (99.0 ± 1.1%) and dilute CO (99.3 ± 0.3%) up to injection flow rate of 6.7 ml/min and 105 ml/min, respectively (Fig 3, Table 5). For dilute CO, which is more representative of environmental samples, the efficiency began to drop at a flow rate > 105 ml/min (Fig. 3) and this limits how fast samples can be introduced to the line. The oxidation efficiency is stable over an oven (Fig. 1, No. 7) temperature range of 247–290 °C for dilute CO and the oven does not oxidize CH_4 passing through at 290 °C (Table 5).

Theoretically, the CO oxidation efficiency depends on both the oxidation of CO to CO_2 in the 290 °C CuO packed oven (Fig. 1, No. 7) and the trapping of CO_2 in the subsequent LN_2 cooled U trap (the CO trap, Fig. 1, No. 8). We tested the trapping efficiency of the CO trap (Fig. 1, No. 8) by injecting CO_2 (60 ml of 2–20% CO_2 in N_2) into the line, leaving the LN_2 off the first trap (Fig. 1, No. 6), and then comparing the CO_2 in the CO trap (Fig. 1, No. 8) with that in the trap where CH_4-derived CO_2 would normally freeze down (Fig. 1, No. 12). These tests showed that the CO trap froze down CO_2 at an efficiency of 99.74 ± 0.29% (n = 6), even at a flow rate > 105 ml/min; thus, the CO oxidation efficiency is solely dependent on the oxidation of CO to CO_2 in the 290 °C oven (Fig. 1, No. 7).

It is important to note that even though the CO trap's (Fig. 1, No. 8) efficiency was adequate for the purpose of CO removal, it was not satisfactory for separating modern OX1-CO_2 from dead CH_4 in the OX1:CH_4 mixed standards prepared on the original line setup (as discussed in Section 3.3). Because there was a 1000-fold difference in the ^{14}C content of the OX1-CO_2 and dead CH_4 in the mixed standards, < 1% of the OX1-CO_2 escaping the CO trap in the initial line setup could explain the high ^{14}C CH_4 values seen for the mixed standards. It is unlikely that the ^{14}C content of CO and CH_4 in environmental samples has a 1000-fold difference

Table 4
Summary of ^{14}C and ^{13}C data from CH_4:OX1-CO_2 mixed standards and OX1-CO_2 in N_2 prepared on the flow-through vacuum line after installation of the multi-loop trap (Fig. 1, No. 6; SD, ± 1σ standard deviation; age = radiocarbon age in kyr).

Storage time (months)	^{14}C OX1-CO_2			^{13}C OX1-CO_2			^{14}C-CH_4			^{13}C-CH_4		
	n	FM	SD	n	‰	SD	n	Age	SD	n	‰	SD
CH_4:OX1-CO_2 mixed standards in N_2												
0	1	1.0389					1	48.8				
0.5	8	1.0340	0.0021	7	−19.3	0.3	8	51.1	0. 8	6	−36.3	0.1
6.5	1	1.0205					1	50.5				
8.7	1	1.0191		1	−19.5		1	48.0		1	−36.3	
OX1-CO_2 in N_2												
0	2	1.0422	0.0003									
0.5	2	1.0404	0.0005									
2.1	3	1.0372	0.0010	1	−19.1							
6.4	3	1.0351	0.0012									

Fig. 3. CO oxidation efficiency vs. injection flow rate for pure CO (left) and dilute 1% CO (right).

Table 5
CO oxidation efficiency of the 290 °C CuO packed oven (Fig. 1, No. 7) under different oven temperatures. The last line shows the amount of CH_4 oxidized alongside CO in the 290 °C oven.

Standard	n	Oven (°C)	Volume (ml)	Injection (ml/min)	Efficiency (% ± 1σ)
Pure CO	5	290	1.6–2.6	⩽6.7	99.0 ± 1.1
Dilute CO	15	290	14–31	⩽105	99.3 ± 0.3
Pure CO	1	247	1.8	6.7	95.3
Dilute CO	2	247	27	54–58	99.4 ± 0.1
Pure CH_4	3	290	2	⩽20	0[a]

[a] When pure CH_4 was injected into the line with the oven at 290 °C, no CO_2 was recovered in the subsequent LN_2 cooled CO trap (Fig. 1, No. 8).
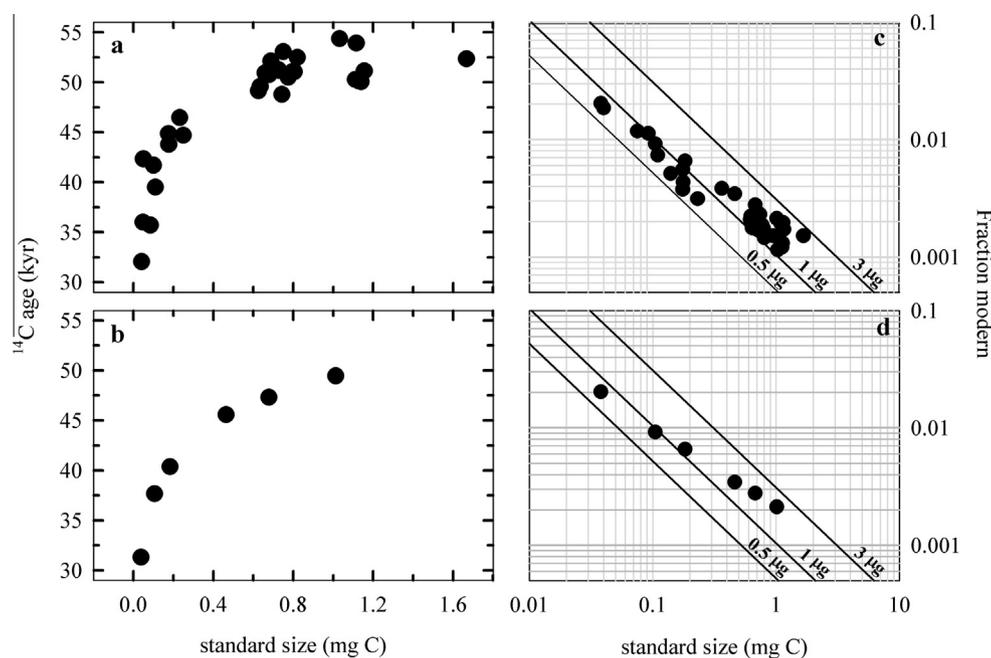
Fig. 4. ^{14}C age and FM of different size aliquots of dead CH_4 (a) and (c) and BD-CO_2 gas (b) and (d) standards prepared on the flow-through vacuum line. For plots (c) and (d), the scale is log base 10 and the solid black lines represent the effect of fixed amounts of modern C background on the dead standard values [based on calculations from Santos et al. (2007)].

(e.g. Petrenko et al., 2013) and CO concentration can be less than CH_4 depending on sample type (e.g. Schmidt and Conrad, 1993; Poissant et al., 2007). With these properties, if 1% of sample CO escaped the CO trap and contaminated the sample CH_4, it should have a minimal effect on the sample's measured ^{14}C CH_4 content.

From tabulating the amount of pure and dilute CO used to test the line's CO oxidation efficiency, we found that the CuO in the 290 °C oven (Fig. 1, No. 7) would be deactivated after it oxidized ca. 19 mg of C from CO. If a sample had a CO concentration of

1 ppm, it would take ca. 37,500 l of sample to deactivate the CuO in the oven. The CuO is regenerated by removing it from the oven trap and baking it in a crucible under room air (900 °C, 2 h). A larger trap containing more CuO would be able to oxidize a greater amount of CO before deactivation. The catalytic ability of CuO to oxidize CO may be dampened by the presence of water (Royer and Duprez, 2011), so we utilize an inline $Mg(ClO_4)_2$ filter (Fig. 1, No. 5) to dry samples before they reach the 290 °C CuO packed oven (Fig. 1, No. 7). A number of factors, including mg C–CO oxi-

dized, water exposure and total time operated since regeneration, likely contribute to the CuO deactivation, so monitoring the CO oxidation efficiency with 1% CO in N_2 run through the flow-through line should be carried out as regular line maintenance.

3.5. Sample volume and concentration

We evaluated the flow-through line for sample volumes of ca. 180 ml with CH_4 and CO_2 concentration of ca. 0.5–1%. This volume and concentration gave ca. 0.5–1 mg C for both CH_4 and CO_2. In order to prepare samples with lower CH_4 and/or CO_2 concentration on the line (i) modern ^{14}C background corrections would need to be adjusted for sample size, (ii) fossil ^{14}C backgrounds would need to be quantified and/or (iii) larger sample volumes may be required.

To investigate the relationship between modern ^{14}C background and sample size, we prepared a series of small dead standards (BD-CO_2 and CH_4 gas; 0.04–0.5 mg C) on the line. The resulting data, along with the 0.5–1 mg C data from above, show that the modern ^{14}C background is inversely proportional to sample size when size drops below 0.5 mg C (Fig. 4a and b; i.e. larger samples dilute the constant background contamination more than smaller ones). Using the isotope mass balance equations outlined by Santos et al. (2007) to evaluate our dead standard data confirmed that the size of the contaminating modern background was constant at ca. 0.0006–0.0011 mg C (Fig. 4c and d). Because of this inverse relationship, the measured ^{14}C content of small dead standards must be used to adjust the modern ^{14}C background for small samples (< 0.5 mg C). Such an adjustment allows ca. 180 ml samples with a CH_4 and CO_2 concentration down to 0.1% (yielding 0.1 mg C) to be prepared on the line. For samples with < 0.1 mg C, we would need to also address the fossil ^{14}C background (Santos et al., 2007). For future work, in addition to addressing the fossil background, we plan to use graphitization techniques that minimize background effects and improve graphitization efficiency with smaller (0.015–0.1 mg C; Khosh et al., 2010) and ultra-small (0.004–0.015 mg C; Xu et al., 2013) samples.

The second option to compensate for low CH_4 and CO_2 concentration is the use of larger sample volumes (> 180 ml). However, the line would require several modifications to handle larger volumes. First, 105 ml/min is the highest injection flow rate appropriate for the line due to the CO oxidation efficiency (Fig. 3 and 1% CO). This translates to longer processing time for larger sample volumes; e.g. it would take ca. 20 min to introduce a 2 l sample. Thus, a larger diameter CO oven is needed to allow efficient oxidation of CO at higher flow rate. Second, introducing larger volume samples to the line via a 60 ml syringe (the largest standard size syringe) would require many injections, which would be inefficient and increase the line background. For larger volumes, techniques for introducing samples from gas canisters (stainless steel or glass) or collapsible gas sample bags (Al or plastic) instead of syringes need to be developed and tested.

3.6. Application to natural samples

Here we present the first depth profiles of ^{14}C CH_4 and ^{14}C CO_2 from soil pore gas in an Arctic peatland. Gas samples were collected over a 2 week period from a fen on North Mountain, near Thule, Greenland (76°32′N, 68°50′W) using PVC gas probes with inner silicone membrane tubes. The membranes allowed CH_4 and CO_2 gas from the soil to diffuse into the inner volume of the gas probes (Jacinthe and Groffman, 2001; Kamman et al., 2001; De Gregorio et al., 2005). Samples were taken from the gas probes with a 60 ml syringe and stored in 2 × 120 ml evacuated glass serum bottles with blue butyl rubber stoppers. The samples were

returned to UC Irvine and prepared for ^{14}C AMS analysis on the flow-through vacuum line.

The $\Delta^{14}C$ CH_4 data showed a gradual decrease with depth (Fig. 5), but ranged from 3.2‰ to 44.4‰ [‰ as defined by Stuiver and Polach (1977)] and were all modern. This indicated that the main component of CH_4 at the site was derived from C fixed within recent decades and not that old C that had been buried and isolated from the atmosphere for millennia. The $\Delta^{14}C$ CH_4 data also correlated with the $\Delta^{14}C$ CO_2 data (Fig. 5), suggesting that CH_4 and CO_2 were derived from a similar C source at the site. Altogether, these data demonstrate both the efficacy of ^{14}C measurements in C cycle studies and for detecting the release of old C from peatlands and other climate sensitive C reservoirs.
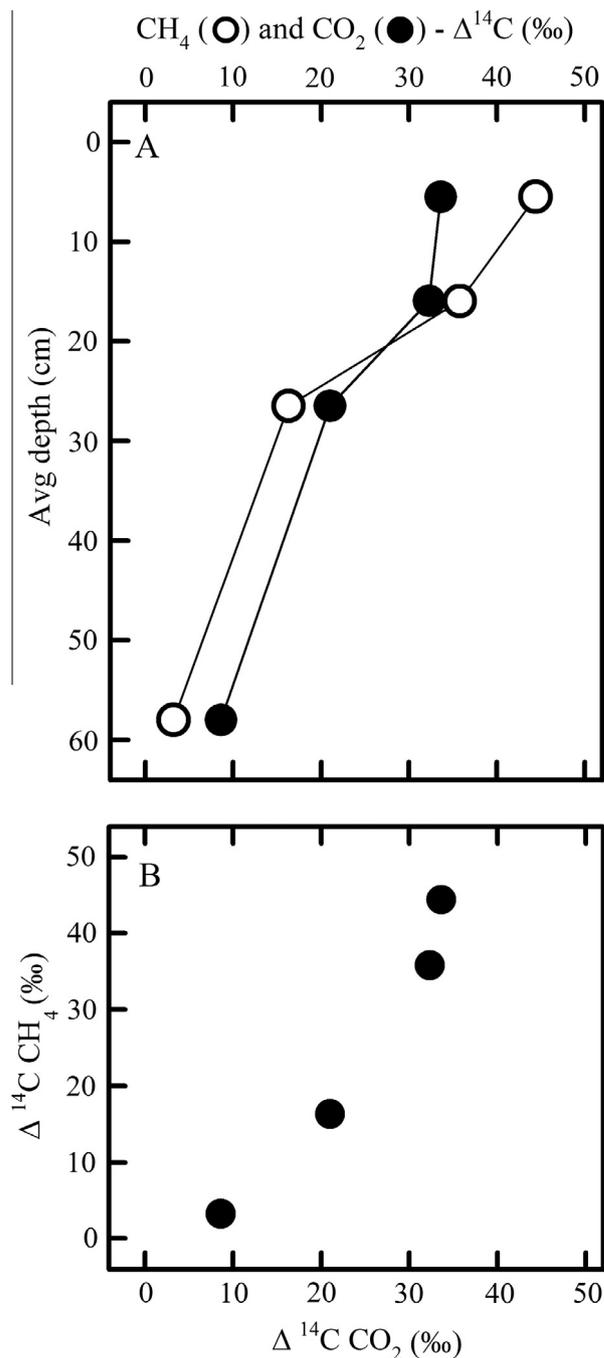

Fig. 5. CH_4 and CO_2 ^{14}C AMS data from Arctic soil pore gas samples.

Northern peatlands store vast amounts of C and may provide a positive feedback if their C stores are impacted by the warming climate (Davidson and Janssens, 2006). In order to obtain accurate future projections of atmospheric CH_4, it is important that C cycling within peatlands is well understood. A small number of C isotope studies (^{14}C and ^{13}C of CH_4 and CO_2) of northern peatlands (e.g. Wahlen et al., 1989; Quay et al., 1991; Chanton et al., 1995, 2008; Chasar et al., 2000; Clymo and Bryant, 2008; Garnett et al., 2011, 2012) have provided insight into the production, consumption and transport pathways of CH_4 and CO_2, and the rate at which they are cycled between reservoirs. These C isotope studies go back more than a decade, but remain incomplete with respect to sample depth resolution, location (e.g. topography, hydraulic conductivity), type of ecosystem and seasonality (Chasar et al., 2000); namely, C cycling patterns in peatlands need to be linked to these local properties. The shortage of data is, in part, due to the challenges and cost associated with ^{14}C CH_4 measurements, both in collecting gas samples from peatlands (Clymo and Bryant, 2008; Garnett et al., 2011) and sample processing in the lab. The rapid and convenient sample preparation method described here should provide more opportunities for ^{14}C CH_4 measurements for peatlands and a variety of other C cycle studies.

4. Conclusions

The flow-through vacuum line described here can reliably allow preparation of CH_4 and CO_2 from environmental samples for isotopic analysis and should help increase the use of ^{14}C CH_4 measurements in C cycle studies. The modern ^{14}C background for CH_4 and CO_2 is satisfactory and consistent, and the precision and accuracy are good. The main advantages of the method are that it (i) is rapid – 1 h for both CH_4 and CO_2, 30 min for CH_4 alone, (ii) completely separates CH_4 and CO_2 while maintaining a low ^{14}C background and (iii) efficiently oxidizes CO to CO_2 for cryogenic removal using a catalytic agent that can be easily regenerated. Further, the system uses UZ air for a carrier gas, which is less expensive than He and safer than pure O_2, yet still provides enough O_2 for CH_4 combustion and maintains a sufficiently low ^{14}C background. The main disadvantage is that, because samples are introduced to the vacuum line via syringe and the maximum allowable injection flow rate is 105 ml/min (due to CO oxidation efficiency), the technique is limited to a small sample volume (ca. 180 ml) with a relatively high concentration of CH_4 and CO_2 (> 0.1%). For future work, we will improve CO oxidation efficiency with a larger diameter CuO packed 290 °C oven and develop techniques for introducing samples via gas canisters and gas sample bags.

Acknowledgements

Associate Editor—**S. Schouten**

References

Alperin, M.J., Reeburgh, W.S., Whiticar, M.J., 1988. Carbon and hydrogen isotope fractionation resulting from anaerobic methane oxidation. Global Biogeochemical Cycles 2, 279–288.

Aravena, R., Wassenaar, L.I., 1993. Dissolved organic carbon and methane in a regional confined aquifer, southern Ontario, Canada: carbon isotope evidence for associated subsurface sources. Applied Geochemistry 8, 483–493.

Chanton, J.P., Whiting, G.J., Showers, W.J., Crill, P.M., 1992. Methane flux from *Peltandra Virginica*: stable isotope tracing and chamber effects. Global Biogeochemical Cycles 6, 15–31.

Chanton, J.P., Bauer, J.E., Glaser, P.A., Siegel, D.I., Kelley, C.A., Tyler, S.C., Romanowicz, E.H., Lazrus, A., 1995. Radiocarbon evidence for the substrates supporting methane formation within northern Minnesota peatlands. Geochimica et Cosmochimica Acta 59, 3663–3668.

Chanton, J.P., Glaser, P.H., Chasar, L.S., Burdige, D.J., Hines, M.E., Siegel, D.I., Tremblay, L.B., Cooper, W.T., 2008. Radiocarbon evidence for the importance of surface vegetation on fermentation and methanogenesis in contrasting types of boreal peatlands. Global Biogeochemical Cycles 22, GB4022, http://dx.doi.org/10.1029/2008GB003274.

Chasar, L.S., Chanton, J.P., Glaser, P.H., Siegealnd, D.I., Rivers, J.S., 2000. Radiocarbon and stable carbon isotopic evidence for transport and transformation of dissolved organic carbon, dissolved inorganic carbon, and CH_4 in a northern Minnesota peatland. Global Biogeochemical Cycles 14, 1095–1108.

Clymo, R.S., Bryant, C.L., 2008. Diffusion and mass flow of dissolved carbon dioxide, methane, and dissolved organic carbon in a 7-m deep raised peat bog. Geochimica et Cosmochimica Acta 72, 2048–2066.

Currie, L.A., Polach, H.A., 1980. Exploratory analysis of the international radiocarbon cross-calibration data; consensus values and interlaboratory error; preliminary note. Radiocarbon 22, 933–935.

Davidson, E.A., Janssens, I.A., 2006. Temperature sensitivity of soil carbon decomposition and feedbacks to climate change. Nature 440, 165–173.

De Gregorio, S., Gurrieri, S., Valenza, M., 2005. A PTFE membrane for the in situ extraction of dissolved gases in natural waters: theory and applications. Geochemistry, Geophysics, Geosystems 6, 1–13.

Dlugokencky, E.J., Nisbet, E.G., Fisher, R., Lowry, D., 2011. Global atmospheric methane: budget, changes. Philosophical Transactions of the Royal Society A 369, 2058–2072.

Fiore, A., Naik, M.V., Spracklen, D.V., Steiner, A., Unger, N., Prather, M., Bergmann, D., Cameron-Smith, P.J., Cionni, I., Collins, W.J., Dalsøren, S., Eyring, V., Folberth, G.A., Ginoux, P., Horowitz, L.W., Josse, B., Lamarque, J.-F., MacKenzie, I.A., Nagashima, T., O'Connor, F.M., Righi, M., Rumbold, S.T., Shindell, D.T., Skeie, R.B., Sudo, K., Szopa, S., Takemurat, T., Zeng, G., 2012. Global air quality and climate. Chemical Reviews 41, 6663–6683.

Gao, P., Xu, X., Zhoua, L., Pack, M.A., Griffin, S., Santos, G.M., Southon, J.R., Liuc, K., 2014. Rapid sample preparation of dissolved inorganic carbon in natural waters using a headspace-extraction approach for radiocarbon analysis on accelerator mass spectrometry. Limnology and Oceanography: Methods 12, 171–190. http://dx.doi.org/10.4319/lom.2014.12.174.

Garnett, M.H., Hardie, S.M.L., Murray, C., 2011. Radiocarbon and stable carbon analysis of dissolved methane and carbon dioxide from the profile of a raised peat bog. Radiocarbon 53, 71–83.

Garnett, M.H., Hardie, S.M.L., Murray, C., 2012. Radiocarbon analysis of methane emitted from the surface of a raised peat bog. Soil Biology and Biochemistry 50, 158–163.

Garnett, M.H., Hardie, S.M.L., Murray, C., Billett, M.F., 2013. Radiocarbon dating of methane and carbon dioxide evaded from a temperate peatland stream. Biogeochemistry 114, 213–223. http://dx.doi.org/10.1007/s10533-012-9804-2.

Hardie, S.M.L., Garnett, M.H., Fallick, A.E., Rowland, A.P., Ostle, N.J., 2005. Carbon dioxide capture using a zeolite molecular sieve sampling system for isotopic studies (^{13}C and ^{14}C) of respiration. Radiocarbon 47, 441–451.

Heimann, M., Reichstein, M., 2008. Terrestrial ecosystem carbon dynamics and climate feedbacks. Nature 451, 289–292.

Hinger, E.N., Santos, G.M., Druffel, E.R.M., Griffin, S., 2010. Carbon isotope measurements of surface seawater from a time-series off Southern California. Radiocarbon 52, 69–89.

Jacinthe, P.A., Groffman, P.M., 2001. Silicon rubber sampler to measure dissolved gases in saturated soils and waters. Soil Biology and Biochemistry 33, 907–912.

Kamman, C., Grünhage, L., Jäger, H.J., 2001. A new sampling technique to monitor concentrations of CH_4, N_2O and CO_2 in air and well-defined depths in soils with varied water potential. European Journal of Soil Science 52, 297–303.

Kessler, J.D., Reeburgh, W.S., 2005. Preparation of natural methane samples for stable isotope and radiocarbon analysis. Limnology and Oceanography: Methods 3, 408–418.

Kessler, J.D., Reeburgh, W.S., Southon, J., Varela, R., 2005. Fossil methane source dominates Cariaco Basin water column methane geochemistry. Geophysical Research Letters 32, L12609.

Kessler, J.D., Reeburgh, W.S., Tyler, S.C., 2006. Controls on methane concentration and stable isotope (δ^2H–CH_4 and $\delta^{13}C$–CH_4) distributions in the water columns of the Black Sea and Cariaco Basin. Global Biogeochemical Cycles 20, GB4004.

Khosh, M.S., Xu, X., Trumbore, S.E., 2010. Small-mass graphite preparation by sealed tube zinc reduction method for AMS ^{14}C measurements. Nuclear Instruments and Methods in Physics Research, Section B 268, 927–930.

Klouda, G.A., Connolly, M.V., 1995. Radiocarbon (^{14}C) measurements to quantify sources of atmospheric carbon monoxide in urban air. Atmospheric Environment 29, 3309–3318.

Kvenvolden, K.A., 1995. A review of the geochemistry of methane in natural gas hydrate. Organic Geochemistry 23, 997–1008.

Le Mer, J., Roger, P., 2001. Production, oxidation, emission and consumption of methane by soils: a review. European Journal of Soil Biology 37, 25–50.

Lowe, D.C., Brenninkmeuer, A.M., Tyler, S.C., Dlugokencky, E.J., 1991. A method for the determination of the isotopic composition of atmospheric methane and its application in the Antarctic. Journal of Geophysical Research 96, 15455–15467.

Mook, W.G., Van Der Plicht, J., 1999. Reporting ^{14}C activities and concentrations. Radiocarbon 41, 227–239.

Myhre, G., Shindell, D., Bréon, F.-M., Collins, W., Fuglestvedt, J., Huang, J., Koch, D., Lamarque, J.-F., Lee, D., Mendoza, B., Nakajima, T., Robock, A., Stephens, G., Takemura, T., Zhang, H., 2013. Anthropogenic and natural radiative forcing. In: Stocker, T.F., Qin, D., Plattner, G.-K., Tignor, M., Allen, S.K., Boschung, J., Nauels, A., Xia, Y., Bex, V., Midley, P.M. (Eds.), Climate Change 2013: The Physical Science Basis. Contributions of Working Group I to the Fifth Assessment Report of the Intergovernmental Panel on Climate Change. Cambridge University Press, Cambridge, United Kingdom and New York, NY, USA, pp. 661–740.

Pack, M.A., Heintz, M.B., Reeburgh, W.S., Trumbore, S.E., Valentine, D.L., Xu, X., Druffel, E.R.M., 2011. A method for measuring methane oxidation rates using low-levels of ^{14}C-labeled methane and accelerator mass spectrometry. Limnology and Oceanography: Methods 9, 245–260.

Petrenko, V.V., Smith, A.M., Brailsford, G., Riedel, K., Hua, Q., Lowe, D., Severinghaus, J.P., Levchenko, V., Bromley, T., Moss, R., Mühle, J., Brook, E.J., 2008. A new method for analyzing ^{14}C of methane in ancient air extracted from glacial ice. Radiocarbon 50, 53–73.

Petrenko, V.V., Severinghaus, J.P., Smith, A.M., Riedel, K., Baggenstos, D., Harth, C., Orsi, A., Hua, Q., Franz, P., Takeshita, Y., Brailsford, G.W., Weiss, R.F., Buizert, C., Dickson, A., Schaefer, H., 2013. High-precision ^{14}C measurements demonstrate production of in situ cosmogenic [14]CH$_4$ and rapid loss of in situ cosmogenic [14]CO in shallow Greenland firn. Earth and Planetary Science Letters 365, 190–197.

Pohlman, J.W., Knies, D.L., Grabowski, K.S., DeTurck, T.M., Treacy, D.J., Coffin, R.B., 2000. Sample distillation/graphitization system for carbon pool analysis by accelerator mass spectrometry (AMS). Nuclear Instruments and Methods in Physics Research, Section B 172, 428–433.

Pohlman, J.W., Bauer, J.E., Canuel, E.A., Grabowski, K.S., Knies, D.L., Mitchell, C.S., Whiticar, M.J., Coffin, R.B., 2009. Methane sources in gas hydrate bearing cold seeps: evidence from radiocarbon and stable isotopes. Marine Chemistry 115, 102–109.

Poissant, L., Constant, P., Pilote, M., Canário, J., O'Driscoll, N., Ridal, J., Lean, D., 2007. The ebullition of hydrogen, carbon monoxide, methane, carbon dioxide and total gaseous mercury from the Cornwall Area of Concern. Science of the Total Environment 381, 256–262.

Prather, M.J., Holmes, C.D., Hsu, J., 2012. Reactive greenhouse gas scenarios: systematic exploration of uncertainties and the role of atmospheric chemistry. Geophysical Research Letters 39, L09803.

Quay, P.D., King, S.L., Stutsman, J., Wilbur, D., Steele, L., Fung, I., Gammon, R., Brown, T.A., Farwell, G., Grootes, P., Schmidt, F., 1991. Carbon isotopic composition of atmospheric CH$_4$: fossil and biomass burning source strengths. Global Biogeochemical Cycles 5, 25–47.

Reeburgh, W.S., 2007. Oceanic methane biogeochemistry. Chemical Reviews 107, 486–513.

Royer, S., Duprez, D., 2011. Catalytic oxidation of carbon monoxide over transition metal oxides. ChemCatChem 3, 24–65.

Sansone, F.J., Popp, B.N., Gasc, A., Graham, A.W., Rust, T.M., 2001. Highly elevated methane in the eastern tropical North Pacific and associated isotopically enriched fluxes to the atmosphere. Geophysical Research Letters 28, 4567–4570.

Santos, G.M., Southon, J.R., Griffin, S., Beaupre, S.R., Druffel, E.R.M., 2007. Ultra small-mass AMS ^{14}C sample preparation and analyses at KCCAMS/UCI Facility. Nuclear Instruments and Methods in Physics Research, Section B 259, 293–302.

Schmidt, U., Conrad, R., 1993. Hydrogen, carbon monoxide, and methane dynamics in Lake Constance. Limnology and Oceanography 38, 1214–1226.

Southon, J.R., Santos, G.M., 2004. Ion source development at KCC AMS, University of California, Irvine. Radiocarbon 46, 33–39.

Southon, J.R., Santos, G.M., 2007. Life with MC-SNICS. Part II: Further ion source development at the Keck carbon cycle AMS facility. Nuclear Instruments and Methods in Physics Research, Section B 259, 88–93.

Spahni, R., Wania, R., Neef, L., Van Weele, M., Pison, I., Bousquet, P., Frankenberg, C., Foster, P.N., Joos, F., Prentice, I.C., van Velthoven, P., 2011. Constraining global methane emissions and uptake by ecosystems. Biogeosciences Discussions 8, 1643–1665.

Steinmann, P., Eilrich, B., Leuenberger, M., Burns, S.J., 2008. Stable carbon isotope composition and concentrations of CO$_2$ and CH$_4$ in the deep catotelm of a peat bog. Geochimica et Cosmochimica Acta 72, 6015–6026.

Stuiver, M., Polach, H.A., 1977. Discussion: reporting ^{14}C data. Radiocarbon 19, 355–363.

Townsend-Small, A., Tyler, S.C., Pataki, D.E., Xu, X., Christensen, L.E., 2012. Isotopic measurements of atmospheric methane in Los Angeles, California, USA: influence of "fugitive" fossil fuel emissions. Journal of Geophysical Research: Atmospheres 177, D07308.

Trumbore, S., 2009. Radiocarbon and soil carbon dynamics. Annual Review of Earth and Planetary Sciences 37, 47–66. http://dx.doi.org/10.1146/annurev.earth.36.031207.124300.

Wahlen, M., Tanaka, N., Henry, R., Deck, B., Zeglen, J., Vogel, J.S., Southon, J., Shemesh, A., Fairbanks, R., Broecker, W., 1989. Carbon-14 in methane sources and in atmospheric methane: the contribution from fossil carbon. Science 245, 286–290.

Whiticar, M.J., 1999. Carbon and hydrogen isotope systematics of bacterial formation and oxidation of methane. Chemical Geology 161, 291–314.

Xu, X., Trumbore, S.E., Zheng, S.H., Southon, J.R., McDuffee, K.E., Luttgen, M., Liu, J.C., 2007. Modifying a sealed tube zinc reduction method for preparation of AMS graphite targets: reducing background and attaining high precision. Nuclear Instruments and Methods in Physics Research, Section B 259, 320–329.

Xu, X., Gao, P., Salamanca, E.G., 2013. Ultra small-mass graphitization by sealed tube zinc reduction method for AMS ^{14}C measurements. Radiocarbon 55, 608–619.

Yusuf, R.O., Noor, Z.Z., Abba, A.H., Hassan, M.A.A., Din, M.F.M., 2012. Methane emission by sectors: a comprehensive review of emission sources and mitigation methods. Renewable and Sustainable Energy Reviews 16, 5059–5070.